Kinetic Mechanism of RGS9-1 Potentiation by R9AP†

Sheila A. Baker,[‡,§] Kirill A. Martemyanov,[§,||] Alexander S. Shavkunov,[‡] and Vadim Y. Arshavsky*[,‡,⊥]

Department of Ophthalmology, Duke University, Durham, North Carolina 27710, Department of Pharmacology, University of Minnesota, Minneapolis, Minnesota 55455, and Department of Neurobiology, Duke University, Durham, North Carolina 27710

Received February 23, 2006; Revised Manuscript Received June 21, 2006

ABSTRACT: The duration of the photoreceptor's response to a light stimulus determines the speed at which an animal adjusts to ever-changing conditions of the visual environment. One critical component which regulates the photoresponse duration on the molecular level is the complex between the ninth member of the regulators of G protein signaling family (RGS9-1) and its partner, type 5 G protein β-subunit (Gβ5L). RGS9-1·Gβ5L is responsible for the activation of the GTPase activity of the photoreceptor-specific G protein, transducin. Importantly, this function of RGS9-1·Gβ5L is regulated by its membrane anchor, R9AP, which drastically potentiates the ability of RGS9-1·Gβ5L to activate transducin GTPase. In this study, we address the kinetic mechanism of R9AP action and find that it consists primarily of a direct increase in the RGS9-1·Gβ5L activity. We further showed that the binding site for RGS9-1·Gβ5L is located within the N-terminal putative trihelical domain of R9AP, and even though this domain is sufficient for binding, it takes the entire R9AP molecule to potentiate the activity of RGS9-1·Gβ5L. The mechanism revealed in this study is different from and complements another well-established mechanism of regulation of RGS9-1·Gβ5L by the effector enzyme, cGMP phosphodiesterase, which is based entirely on the enhancement in the affinity between RGS9-1·Gβ5L and transducin. Together, these mechanisms ensure timely transducin inactivation in the course of the photoresponse, a requisite for normal vision.

The temporal resolution of vision is crucially dependent on the balance between the rates at which the key components of the visual signaling cascade are activated and inactivated (see ref *1* for a recent review). Transducin, the G protein mediating phototransduction, is activated by photoexcited rhodopsin which catalyzes the GDP/GTP exchange on the transducin α-subunit (*2*) and then deactivated through GTP hydrolysis stimulated by the GTPase activating protein, the short splice variant of RGS9, RGS9-1[1] (*3*). The rate of transducin activation determines the sensitivity of the light response, whereas the inactivation rate determines the kinetics of response recovery, with both processes accomplished within a fraction of a second. In photoreceptors, RGS9-1 is present in a complex with its constitutive partner, the long splice variant of Gβ5, Gβ5L (*4*), and anchored to the membrane by a SNARE-like protein, R9AP (*5*).

The role of R9AP within the GTPase activating complex is more extensive than merely holding the complex on the surface of the photoreceptor membranes. R9AP targets the RGS9-1·Gβ5L complex to the photoreceptor outer segment, the organelle where visual signal transduction takes place (*6*), regulates the expression level and post-translational stability of RGS9-1·Gβ5L (*7*), and dramatically enhances the ability of RGS9-1·Gβ5L to stimulate the GTPase activity of transducin (*6*, *8*, *9*). In fact, transducin inactivation on the physiological subsecond time scale can be accomplished only when RGS9-1·Gβ5L is bound to R9AP.

In this study, we address the mechanism by which R9AP stimulates the activity of RGS9-1·Gβ5L. A combination of a kinetic analysis of transducin GTPase and pull-down assays of protein−protein interactions revealed that this stimulation consists primarily of enhancement of the catalytic efficiency of RGS9-1·Gβ5L, which causes an ∼16-fold increase in the rate of transducin GTPase. An additional contribution results from an ∼2-fold enhancement of the affinity of RGS9-1·Gβ5L for transducin. We further identified that the N-terminal domain of R9AP, predicted to form a trihelical structure, serves as the binding site for RGS9-1·Gβ5L. This domain alone efficiently competes with R9AP for binding to RGS9-1·Gβ5L, but it is not sufficient for RGS9-1·Gβ5L activation.

EXPERIMENTAL PROCEDURES

Purification of Photoreceptor Membranes and Native Proteins. Bovine rod outer segments were isolated from frozen retinas as described in ref *10*. Urea-treated rod outer

† This work was supported by NIH Grant EY-12859 (V.Y.A.), NIH core grant for vision research (EY-14104) to the Massachusetts Eye and Ear Infirmary, and NIH core grant for vision research (EY-5722) to Duke University. V.Y.A. is a recipient of a Senior Investigator Award from Research to Prevent Blindness, Inc.

* To whom correspondence should be addressed: Department of Ophthalmology, Duke University Medical Center, 5008 AERI, 2351 Erwin Rd., Durham, NC 27710. Phone: (919) 668-5391. Fax: (919) 684-8829. E-mail: vadim.arshavsky@duke.edu.

‡ Department of Ophthalmology, Duke University.

§ These authors contributed equally to this work.

|| University of Minnesota.

⊥ Department of Neurobiology, Duke University.

[1] Abbreviations: RGS, regulator of G protein signaling; RGS9-1, short splice variant of the ninth member of the RGS protein family; Gβ5L, long splice variant of the type 5 G protein β-subunit; R9AP, RGS9-1 anchor protein; uROS, rod outer segment membranes treated with urea; V8-uROS, uROS treated with protease V8; PDEγ-(63−87), peptide corresponding to residues 63−87 of the γ-subunit of type 6 cGMP phosphodiesterase; GTPγS, guanosine 5′-*O*-(thiotriphosphate); SNARE, soluble *N*-ethylmaleimide-sensitive factor attachment protein receptor; R7BP, RGS R7 subfamily binding protein.

10.1021/bi060376a CCC: $33.50
Published on Web 08/09/2006

segments lacking RGS9-1·Gβ5L activity (uROS) but preserving R9AP were prepared according to the method described in ref *11*. uROS containing inactivated R9AP (V8-uROS) were obtained by proteolytic treatment of uROS with Glu-C protease (Protease V8, Sigma) as described in ref *8*. The rhodopsin concentration in all membrane preparations was determined spectrophotometrically using the ϵ_{500} of 40 000 (*12*). Transducin was purified from bovine rod outer segments as described in ref *13*, and its concentration was determined on the basis of the maximum amount of rhodopsin-catalyzed GTPγS binding performed as described in ref *2*.

Cloning of R9AP Fragments. R9AP fragments were generated by PCR cloning using the previously cloned mouse R9AP gene as the template (*6*). Forward and reverse primers were designed to add an NdeI and EcoRI restriction site, respectively. The PCR products were gel purified, digested with NdeI and EcoRI, and ligated into a pGEX2T vector downstream from the GST coding sequence and a linker encoding a hexahistidine tag flanked by BamHI and NdeI restriction sites. All constructs were verified by sequencing. The construct encoding R9AP residues 1−206 was designated R9APΔTM; that encoding residues 1−132 as H1,2,3,+Linker; that encoding residues 1−110 as H1,2,3; that encoding residues 1−29 as H1; that encoding residues 1−68 as H1,2; that encoding residues 31−206 as ΔH1; that encoding residues 64−206 as ΔH1,2; and that encoding residues 112−206 as SNARE+Linker.

Expression and Purification of Recombinant Proteins. His-tagged RGS9-1·Gβ5L was expressed and purified from Sf-9 cells infected with recombinant baculoviruses as previously described (*14*). The His-tagged R9AP was purified from *Escherichia coli* essentially as described in ref *9*, the exception being that 1% octyl glucoside was used instead of 4% sodium cholate. The GST−R9AP fragments were purified from *E. coli* (BL21) cells transformed with the constructs described above. Cells were disrupted by sonication in buffer containing 300 mM NaCl, 2.7 mM KCl, 10 mM Na_2HPO_4, and 1.8 mM KH_2PO_4 (pH 7.3) supplemented with a Complete Protease Inhibitor cocktail (Roche Diagnostics). The lysates were clarified by centrifugation at 55000*g* for 1 h, and supernatants were incubated with Glutathione−Sepharose 4 Fast Flow beads (Amersham Biosciences) for 2 h at 4 °C, washed in binding buffer, and eluted with buffer containing 10 mM glutathione. Glutathione was removed by gel filtration of the purified fragments into a storage buffer containing 25 mM Tris (pH 7.8), 300 mM NaCl, and 20% glycerol. Proteins were concentrated using Centricon centrifugal filter devices (Millipore). Sf-9 cell membranes containing recombinant R9AP were prepared as described previously (*6*).

GTPase Assays in the Presence of Rhodopsin. Transducin GTPase activity was measured using either multiple-turnover ([GTP] > [transducin]) or single-turnover ([GTP] < [transducin]) assays as described in detail in ref *15*. Assays were conducted at room temperature (22−24 °C) in a buffer containing 100 mM NaCl, 8 mM $MgCl_2$, 10 mM Tris·HCl (pH 7.8), and 1 mM DTT (250 mM NaCl was used in the experiments described in Figure 2B). Illuminated uROS or V8-uROS were used as the source of photoexcited rhodopsin required for transducin activation. The reaction was started by the addition of 10 μL of [γ-^{32}P]GTP at the desired concentration (final concentration of 200 μM in multiple-turnover assays and 0.2 μM in single-turnover assays; approximately 10^5 dpm/sample) to 20 μL of membranes reconstituted with appropriate proteins. The reaction was stopped by the addition of 100 μL of 6% perchloric acid. $^{32}P_i$ formation was measured with activated charcoal. Because high-efficiency interactions between RGS9-1·Gβ5L and transducin require the presence of transducin's effector, the γ-subunit of cGMP phosphodiesterase (*16*), we conducted all GTPase experiments in the presence of the C-terminal peptide from this subunit, PDEγ-(63−87). This peptide has been shown to completely substitute for the full-length phosphodiesterase γ-subunit in this assay (*16*, *17*). All data fitting and statistical analyses were performed using SigmaPlot, version 9.

Membrane-Free GTPase Assay. A version of the single-turnover assay allowing for the measurement of transducin GTPase activity in the absence of membranes was adapted from ref *18* with major modifications. Binding of [γ-^{32}P]-GTP to transducin was performed on ice for 10 min in a reaction mixture including 4.5 μM transducin, 6 M [γ-^{32}P]-GTP (10 μCi), and uROS (20 μM rhodopsin) in a buffer containing 10 mM Tris-HCl (pH 7.8), 100 mM NaCl, 20 mM EDTA, and 1 mM DTT. After centrifugation at 75000*g* (15 min at 2 °C), the supernatant (50 μL) was passed through a 700 μL protein desalting spin column (Pierce Biotechnology) pre-equilibrated with a buffer containing 50 mM HEPES (pH 7.5), 100 mM NaCl, 0.05% decaethylene glycol monododecyl ether ($C_{12}E_{10}$) detergent (Sigma), 5 μg/mL bovine serum albumin, 20 mM EDTA, and 1 mM DTT. The eluate was diluted 3-fold with a buffer containing 10 mM Tris-HCl (pH 7.8), 100 mM NaCl, 5 mM EDTA, and 1 mM DTT. The reaction was started by the addition of 10 μL of this solution containing the GTP-bound transducin to 20 μL of the buffer containing 100 mM NaCl, 8 mM $MgCl_2$, 20 mM Tris-HCl (pH 8.0), 1 mM DTT, 25 μM PDEγ-(63−87), and 1 μM RGS9-1·Gβ5L. The reaction was terminated by the addition of 100 μL of 6% perchloric acid, and the amount of released $^{32}P_i$ was determined using activated charcoal.

Pull-Down Assays. Transducin pull-down assays were conducted as described in detail in ref *15* with minor modifications. Ni−NTA agarose beads (Qiagen, 10 μL) were equilibrated with a binding buffer containing 20 mM Tris-HCl (pH 7.8), 100 mM $NaCl_2$, 2 mM $MgCl_2$, 20 mM imidazole, 0.25% lauryl sucrose, and 50 μg/mL BSA. Recombinant His-tagged RGS9-1·Gβ5L was attached to the beads by being incubated on ice for 20 min at a concentration of 5 μM in a final volume of 50 μL. This amount of RGS9-1·Gβ5L was sufficient to saturate the binding capacity of the beads. The beads were washed and resuspended in 50 μL of buffer containing either 0.7, 3.6, or 18 μM transducin and 15 M PDEγ-(63−87) peptide which is required for the high-affinity transducin−RGS9-1·Gβ5L interaction. When needed, the binding buffer also included 10 mM NaF and 30 μM $AlCl_3$ generating AlF_4^- required for transducin to assume its active conformation that is competent to interact with RGS proteins. R9AP (5 μM) was added when needed. Samples were incubated on ice for 20 min. The beads were washed in the presence of both PDEγ-(63−87) and, when needed, AlF_4^- to preserve high-affinity interaction. Bound transducin was eluted from the beads with

SDS−PAGE sample buffer and analyzed by Western blotting using rabbit anti-transducin antibody (K-20 from Santa Cruz Biotechnology) and the LI-COR Odyssey Infrared Imaging System.

For the GST pull-down assays, Glutathione−Sepharose 4 Fast Flow beads (Amersham Biosciences) were preincubated in 10 mg/mL BSA for 1 h, washed, and resuspended in a binding buffer containing PBS supplemented with 300 mM NaCl, 1% NP-40, and 50 μg/mL BSA; 2 μg of purified GST-tagged R9AP deletion mutants (see above) was incubated with 30 μL of beads for 1 h at 4 °C with rotation. The beads were washed three times with 500 μL of binding buffer and resuspended in 500 μL of buffer containing 0.2 μM His-tagged RGS9-1·Gβ5L. After being incubated for 1 h at 4 °C with rotation, the beads were washed four times with 500 μL of binding buffer, and the bound proteins were eluted with SDS−PAGE sample buffer. RGS9-1 was analyzed by Western blotting using sheep anti-RGS9c antibody (*4*), and GST fusion proteins were detected with mouse anti-GST antibodies (B-14; Santa Cruz Biotechnology).

RESULTS

The Regulation of RGS9-1·Gβ5L by R9AP Consists Primarily of Catalytic Enhancement. In the first series of experiments, we tested whether R9AP activates RGS9-1·Gβ5L by enhancing its affinity for transducin or by increasing the catalytic rate of GTP hydrolysis. We used the kinetic approach developed in our previous studies (*16*) (see ref *15* for a review) where steady-state GTPase assays were conducted at a relatively small fixed concentration of RGS9-1·Gβ5L in the presence of various concentrations of transducin and excess GTP. The data were analyzed by the Michaelis−Menten approach in which RGS9-1·Gβ5L is considered the enzyme and transducin the substrate. The affinity of RGS9-1·Gβ5L for transducin is reflected by the value of K_m, whereas the maximal turnover rate of RGS9-1·Gβ5L (the number of transducin molecules whose GTPase activity can be activated by a RGS9-1·Gβ5L molecule per second) is reflected by the value of k_{cat}.

A typical experiment addressing the effect of R9AP on RGS9-1·Gβ5L activity is shown in Figure 1. In one case, RGS9-1·Gβ5L was reconstituted with photoreceptor membranes containing native R9AP but lacking endogenous RGS9-1·Gβ5L (uROS); in another case, it was reconstituted with membranes in which R9AP was inactivated by proteolysis (V8-uROS). The Michaelis analysis of the data for nonactivated RGS9-1·Gβ5L yielded a K_m value of 7.9 μM transducin and a k_{cat} value of 3.2 s^{-1} (based on the V_{max} of 0.49 μM GTP/s and a RGS9-1·Gβ5L concentration of 0.15 μM). The corresponding calculation of K_m and k_{cat} for the R9AP-bound RGS9-1·Gβ5L, described in detail in the next paragraph, yielded a K_m value of 3.6 μM transducin and a k_{cat} value of 43 s^{-1}.

The analysis of the data for R9AP-bound RGS9-1·Gβ5L was somewhat more complex than that for free RGS9-1·Gβ5L because in our experimental design both species were present in the assay. This design was chosen so that the total concentration of RGS9-1·Gβ5L was identical under both conditions and yet was sufficiently high to ensure reliable measurements of the low basal activity of free RGS9-1·Gβ5L. This ensured that the only variable was the type of membrane that was used (uROS vs V8-uROS). Consequently, the RGS9-1·Gβ5L concentration exceeded the content of R9AP in uROS. We determined the fraction of R9AP-bound RGS9-1·Gβ5L by measuring the amount of binding sites within uROS used in the assay. This was accomplished by analyzing the dependency of RGS9-1·Gβ5L activity on its concentration at a fixed amount of uROS, as described previously (*8*). As shown in Figure 2, this activity increases sharply and then continues to rise at a much lower rate after reaching a breaking point. This breaking point corresponds to the amount of R9AP within uROS capable of binding RGS9-1·Gβ5L. The data averaged from two experiments (Figure 2A) showed this amount to be equal to 0.93 ± 0.14 nmol of R9AP/μmol of rhodopsin, consistent with previous estimates (*8*, *9*). Therefore, the overall RGS9-1·Gβ5L activity measured with uROS containing 50 μM rhodopsin (Figure 1) originated from 0.047 μM R9AP-bound and 0.103 μM free RGS9-1·Gβ5L. Therefore, the kinetic parameters of activated RGS9-1·Gβ5L could be determined by fitting the data with the following equation:

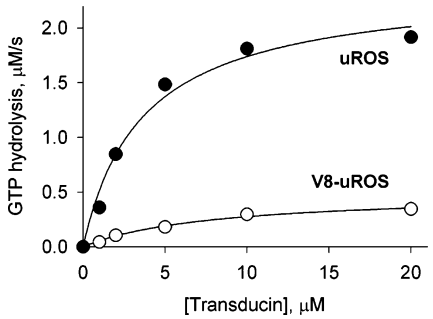

FIGURE 1: Michaelis analysis of the regulation of RGS9-1·Gβ5L activity by native R9AP. Transducin GTPase activity was measured in multiple-turnover assays in reaction mixtures containing 150 nM RGS9-1·Gβ5L, 50 μM PDEγ-(63−87), 200 μM GTP, transducin at the indicated concentrations, and either uROS (●) or V8-uROS (○) each containing 60 μM rhodopsin. The reaction was started by the addition of GTP and terminated after 20 s with perchloric acid (see Experimental Procedures). The basal GTPase activity of transducin equal to 0.072 μM GTP (μM transducin)$^{-1}$ s^{-1} was measured in an independent experiment and subtracted from all points. The data were fitted with hyperbolas yielding the following values: K_m = 7.9 μM and V_{max} = 0.49 μM/s for V8-uROS and K_m = 3.6 μM and V_{max} = 2.4 μM/s for uROS. The data are taken from one of two experiments conducted with uROS and one of three experiments conducted with V8-uROS.

$$V = \frac{k_{cat1}E_1T}{K_{m1} + T} + \frac{k_{cat2}E_2T}{K_{m2} + T} \quad (1)$$

where V is the overall rate of GTP hydrolysis, the first term represents the activity of R9AP-bound RGS9-1·Gβ5L, the second term represents the activity of free RGS9-1·Gβ5L, T is the concentration of transducin, and E_1 and E_2 are the concentrations of bound and free RGS9-1·Gβ5L, respectively. On the basis of the direct measurements described above, we fixed the values of E_1 and E_2 at 0.047 and 0.103 μM, respectively, and k_{cat2} and K_{m2} at 3.2 s^{-1} and 7.9 μM, respectively. This resulted in a k_{cat1} of 43 s^{-1} and a K_{m1} of 3.6 μM transducin for the R9AP-bound fraction of RGS9-1·Gβ5L.

Averaging data from three experiments using V8-uROS and two experiments using uROS indicated that free

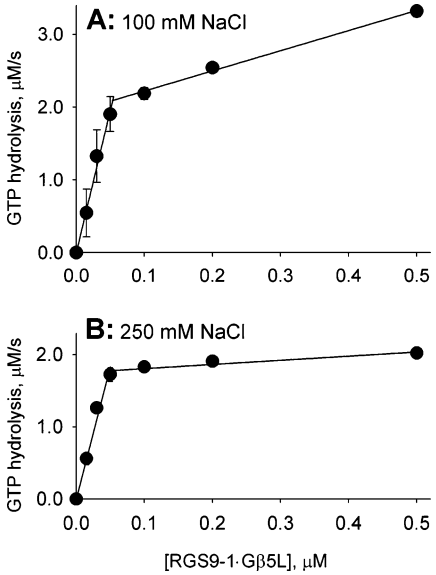

FIGURE 2: Biphasic dependency of transducin GTPase activity on RGS9-1·Gβ5L concentration in the presence of uROS at low and high salt concentrations. Multiple-turnover transducin GTPase assays were performed with uROS containing 60 μM rhodopsin and 20 μM transducin as described in the legend of Figure 1. Experiments in panel A were conducted in the presence of 100 mM NaCl and experiments in panel B in the presence of 250 mM NaCl. Each data set was averaged from two experiments and fitted with two straight lines with slopes of 39 ± 6 and 2.7 ± 0.2 s^{-1} (A) and 35 ± 3 and 0.58 ± 0.1 s^{-1} (B). Error bars indicate the standard error of the mean (note that for many points the bars are smaller than the symbols).

RGS9-1·Gβ5L stimulates transducin GTPase with a k_{cat} of 2.3 ± 0.5 s^{-1} and a K_m of 7.9 ± 2.7 μM (SEM), whereas R9AP-bound RGS9-1·Gβ5L stimulates transducin GTPase with a k_{cat} of 38 ± 5 s^{-1} and a K_m of 3.4 ± 0.2 μM. Therefore, the major effect of R9AP on the ability of RGS9-1·Gβ5L to stimulate transducin GTPase consists of an ~16-fold increase in the value of k_{cat}. A relatively small additional effect of R9AP on the activity of RGS9-1·Gβ5L consisted of a just >2-fold reduction in its K_m for transducin.

The conclusion that the stimulating effect of R9AP is based primarily on the increasing k_{cat} was confirmed in an additional experiment using recombinant R9AP expressed within the membranes of Sf-9 cells, a preparation previously characterized in ref *6*. Membranes were reconstituted with recombinant RGS9-1·Gβ5L, transducin, GTP, and V8-uROS as the source of rhodopsin required for transducin activation (Figure 3). Because the amount of R9AP was in excess of the amount of RGS9-1·Gβ5L, all RGS9-1·Gβ5L was membrane-bound and the standard Michaelis analysis was applied. The K_m value was determined to be 3.9 ± 0.06 μM (SEM, $n = 2$), essentially indistinguishable from the corresponding parameter obtained using native R9AP (Figure 1) and 2-fold lower than that for nonactivated RGS9-1·Gβ5L. The value of k_{cat} was determined to be 11.1 ± 0.7 s^{-1}, 5-fold higher than that for nonactivated RGS9-1·Gβ5L. Note that the overall level of activation of RGS9-1·Gβ5L by recombinant R9AP was lower than by the native R9AP. Although the reasons remain unknown and might relate to either deficiencies in the folding of the recombinant protein or effects of specific membrane microenvironments, this is consistent with previous reports using recombinant R9AP (*6*, *9*). Once again, these data confirm that the major effect of R9AP on RGS9-1·Gβ5L is to enhance the catalytic efficiency of RGS9-1·Gβ5L rather than its affinity for transducin.

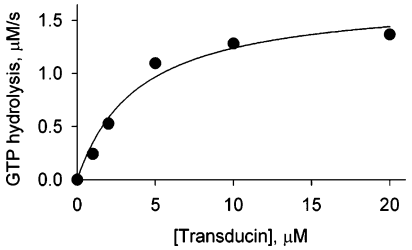

FIGURE 3: Michaelis analysis of the regulation of RGS9-1·Gβ5L activity by recombinant R9AP. Transducin GTPase activity was measured as described in the legend of Figure 1 in the presence of 60 μM V8-uROS and Sf-9 cell membranes containing 3 μM recombinant R9AP. The basal GTPase activity of transducin was subtracted from all points as in Figure 1. The data taken from one of two similar experiments are fitted by a hyperbola yielding the following values: $K_m = 3.9$ μM and $V_{max} = 1.72$ μM/s.

Control Experiment: The Lack of Appreciable R9AP in V8-uROS. V8-uROS are an extremely useful tool for studying the properties of free RGS9-1·Gβ5L due to the lack of endogenous R9AP activity. The latter was originally established by demonstrating that these membranes lack the ability to bind RGS9-1·Gβ5L (*8*). To further verify that V8-uROS did not retain trace amounts of R9AP or did not influence RGS9-1·Gβ5L activity nonspecifically in the experiments presented in Figures 1 and 3, we developed an assay that enabled us to directly monitor the activity of RGS9-1·Gβ5L in the presence or absence of this membrane preparation. We took advantage of the single-turnover approach originally developed for studying the GTPase activity of other G protein subunits (reviewed in ref *18*). It is based on the property of G protein α-subunits to bind GTP in the absence of Mg^{2+} but hydrolyzing it only when Mg^{2+} is present. Typically, a G protein α-subunit is incubated with radiolabeled GTP at high EDTA concentrations to allow spontaneous nucleotide exchange, and then GTP hydrolysis is initiated by the addition of Mg^{2+}. However, to apply this method to the study of transducin, we had to account for its spontaneous rate of nucleotide exchange being orders of magnitude slower than in other G proteins, such as G_o or G_i (*19*−*21*). We therefore modified the assay to first charge transducin with GTP in the presence of rhodopsin but without Mg^{2+}, then to remove the rhodopsin-containing membranes and excess GTP, and finally to initiate the single-turnover GTPase reaction by the addition of Mg^{2+} (see Experimental Procedures for a detailed protocol). The data shown in Figure 4 indicate that RGS9-1·Gβ5L stimulated transducin GTPase in this membrane-free assay and that the addition of V8-uROS had no reliable effect on this activity. At the same time, a control experiment indicated that uROS caused robust RGS9-1·Gβ5L potentiation. In summary, these data indicate that the presence of V8-uROS did not affect the activity of soluble RGS9-1·Gβ5L in our experiments.

The Activity of Soluble But Not R9AP-Bound RGS9-1·Gβ5L is Dependent on Salt Concentration. There is a certain discrepancy between the data from Figure 2A and those previously reported from a virtually identical experiment conducted at a higher salt concentration (Figure 6 from ref *8*). The slopes of the first phases and the positions of the breaking points are nearly identical, but the slope of the second phase, reflecting the activity of soluble RGS9-1·

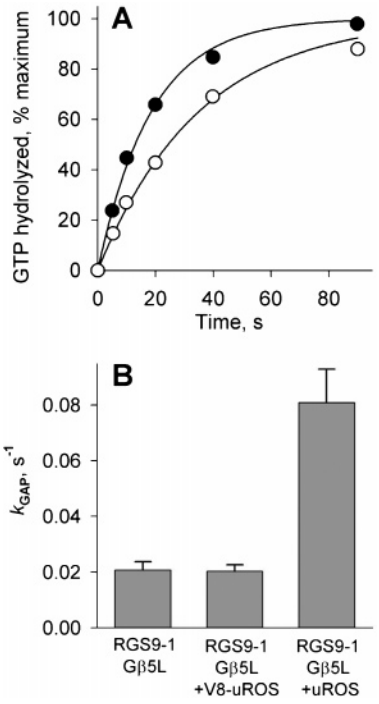

FIGURE 4: Stimulation of transducin GTPase activity by RGS9-1·Gβ5L in the absence of membranes. (A) Single-turnover measurements of transducin GTPase activity in the absence of membranes were conducted with (●) or without (○) 1 μM RGS9-1·Gβ5L as described in Experimental Procedures. The time courses of the GTP hydrolysis were fitted by single exponents, yielding GTPase rate constants of 0.060 ± 0.003 s^{-1} with RGS9-1·Gβ5L and 0.032 ± 0.002 s^{-1} without RGS9-1·Gβ5L. The data were taken from one of two similar experiments. (B) The measurements of activity of RGS9-1·Gβ5L in the membrane-free single-turnover GTPase assay were conducted as described for panel A and after the addition of V8-uROS or uROS containing 20 μM rhodopsin. k_{GAP} is calculated as the difference between the rates of transducin GTPase activity in the presence of RGS9-1·Gβ5L and the basal transducin GTPase activity. The data were taken from the average of two independent experiments; error bars represent the standard error of the mean.

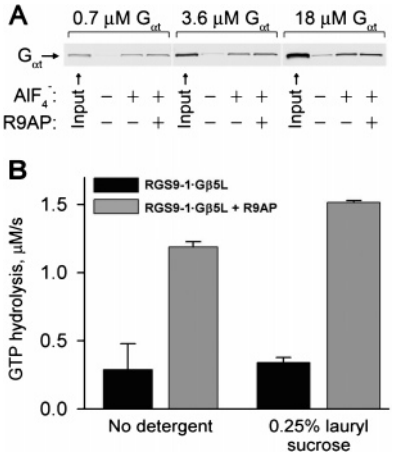

FIGURE 5: R9AP does not significantly affect the interaction between RGS9-1·Gβ5L and transducin in pull-down assays. (A) RGS9-1·Gβ5L immobilized on Ni-NTA agarose beads was incubated with 0.7, 3.6, or 18 μM transducin subunit ($G_{\alpha t}$) activated by AlF_4^- as described in Experimental Procedures. R9AP (5 μM) was added where indicated. The amount of $G_{\alpha t}$ retained on the beads was detected by Western blotting. The absence of AlF_4^- serves as a control for nonspecific binding of nonactivated $G_{\alpha t}$. The lanes marked input were loaded with 10% of the amount of transducin added to the beads. (B) Control experiment confirming the preservation of R9AP activity upon its solubilization by lauryl sucrose. Multiple-turnover GTPase assays were performed as described in the legend of Figure 3 using 20 μM transducin, 0.5 μM RGS9-1·Gβ5L, 20 μM V8-uROS, and, where indicated, Sf-9 cell membranes containing 3 μM recombinant R9AP either intact or solubilized in 0.25% lauryl sucrose. The data are taken from one of two similar experiments.

Gβ5L, is significantly higher in experiments conducted in the presence of 100 mM (now) versus 250 mM NaCl (previously). To directly test whether the salt concentration is the sole reason for this discrepancy, we reproduced the experiment at both NaCl concentrations using the same preparation of membranes and proteins (Figure 2A,B). Indeed, the only difference was the activity of free RGS9-1·Gβ5L, which was nearly 5-fold higher at 100 mM NaCl. This observation allows us to explain why the overall degree of activation of RGS9-1·Gβ5L by R9AP which we reported earlier (~70-fold) was larger than what we observe now (~15-fold). It also explains in part why Hu and colleagues (*9*), who used 100 mM NaCl, observed a lower degree of activation of RGS9-1·Gβ5L by R9AP than we did.

Pull-Down Assays Do Not Reveal a Significant Effect of R9AP on the Affinity Between RGS9-1·Gβ5L and Activated Transducin. Independent evidence that binding of RGS9-1·Gβ5L to R9AP does not cause a major change in its affinity for transducin was obtained in pull-down assays with recombinant RGS9-1·Gβ5L immobilized on Ni−NTA agarose beads (Figure 5A). We used a broad range of transducin concentrations, less than, equal to, and greater than the K_m value for R9AP-activated RGS9-1·Gβ5L (see Figure 1). The retention of activated transducin on these beads was only slightly enhanced by the addition of R9AP (up to ~1.6-fold) at the lower transducin concentrations, with no effect observed at the highest concentration that was tested. This effect was even smaller than the 2.3-fold reduction in the K_m documented in Figure 1, indicating that the latter may originate in part from accumulation of transducin on the membrane surface, rather than being a consequence of direct protein−protein interactions.

Because the pull-down assays were conducted with R9AP solubilized in the detergent lauryl sucrose, we had to verify that R9AP retained full activity under these conditions. This was directly tested by comparing the abilities of membrane-bound and detergent-solubilized recombinant R9AP to activate RGS9-1·Gβ5L. No significant change was found, and in fact, lauryl sucrose caused a small increase in the GTPase activity we measured (Figure 5B).

The N-Terminal Trihelical Bundle of R9AP is Required for Binding to RGS9-1·Gβ5L. We next determined which domain(s) of R9AP is required for binding to RGS9-1·Gβ5L. R9AP belongs to the extended family of SNARE proteins, and its domain composition most closely resembles that of syntaxins (*6*, *22*). As illustrated in Figure 6A, the N-terminus of R9AP contains three immediately adjacent predicted α-helices followed by another helix containing the SNARE homology domain and the C-terminal transmembrane domain. An earlier report indicated that the transmembrane domain does not participate in the interaction with RGS9-1·Gβ5L (*9*). Therefore, we generated a series of deletion constructs from the cytoplasmic portion of the R9AP molecule and tested their ability to bind RGS9-1·Gβ5L. As

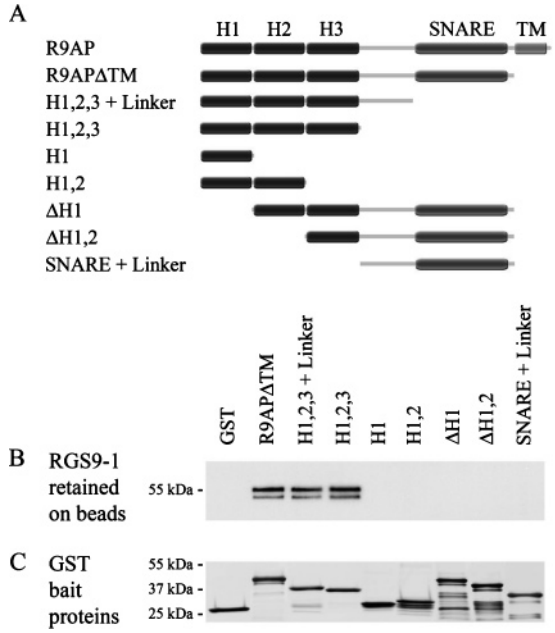

FIGURE 6: The trihelical domain of R9AP is required for RGS9-1·Gβ5L binding. (A) Schematic of the R9AP domain composition and the deletion constructs used in this study. Domains are shown as rectangles with the following abbreviations: H1−H3, first, second, and third putative helix, respectively, from the N-terminus; SNARE, SNARE homology domain; TM, transmembrane domain; Linker, region connecting the three N-terminal helices and the SNARE homology domain (see Experimental Procedures for exact boundaries of each construct). Each construct contained an N-terminal GST tag. (B) Pull-down assays in which GST or GST−R9AP deletion constructs were bound to glutathione−sepharose beads and incubated with recombinant RGS9-1·Gβ5L were performed as described in Experimental Procedures. The amount of bound RGS9-1·Gβ5L was detected by Western blotting using anti-RGS9 antibodies. Note that the lower band detected by the anti-RGS9 antibody is a previously described degradation product of RGS9-1 commonly seen in preparations of recombinant RGS9-1·Gβ5L (*8*, *35*). (C) The amount of bait GST-tagged proteins eluted from the beads was probed with an anti-GST antibody to confirm their similar loading. The lane markings are the same as in panel B. The highest-molecular mass band in each lane corresponds to the expected molecular mass of the respective full-length fusion protein, and the lower-molecular mass bands present in some samples represent degradation products. The data represent one of at least three experiments for each R9AP deletion construct.

shown in Figure 6B, all constructs containing the three N-terminal helices bound RGS9-1·Gβ5L with similar efficiencies. Any further fragmentation of this trihelical bundle resulted in a complete loss of RGS9-1·Gβ5L binding. The constructs containing the SNARE homology domain alone or in combination with incomplete trihelical bundles did not bind RGS9-1·Gβ5L either. These data indicate that the trihelical bundle alone is both necessary and sufficient for binding RGS9-1·Gβ5L. The fact that various perturbations of this domain resulted in a complete loss of binding suggests that it is likely to be folded as a single structural unit which has been shown for the N-terminus of syntaxin (*23*, *24*).

The Trihelical Domain of R9AP Prevents Activation of RGS9-1·Gβ5L by R9AP. It has been reported that R9AP lacking the transmembrane domain could not stimulate the activity of RGS9-1·Gβ5L (*9*). We confirmed this observation (data not shown) and also found that the trihelical domain, sufficient for the interaction with RGS9-1·Gβ5L, also did not affect RGS9-1·Gβ5L basal activity (Figure 7; see bars with V8-uROS). At the same time, this domain completely prevented the activation of RGS9-1·Gβ5L by native R9AP (Figure 7; see bars with uROS). The RGS9-1·Gβ5L activity detected in the presence of a saturating concentration of the trihelical domain is identical to the activity of soluble RGS9-1·Gβ5L (compare the first and last bars in Figure 7), which is consistent with the trihelical domain competing with R9AP for RGS9-1·Gβ5L binding without interfering with RGS9-1·Gβ5L basal activity.

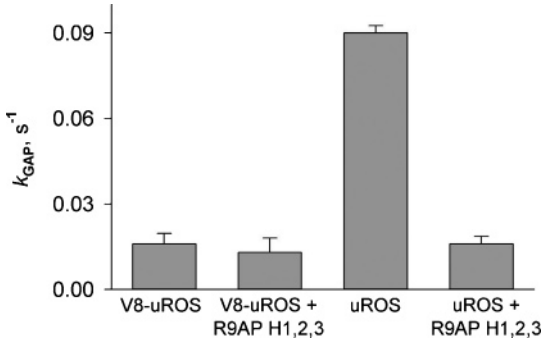

FIGURE 7: The trihelical domain of R9AP prevents the activation of RGS9-1·Gβ5L by R9AP. Single-turnover GTPase assays were conducted as described in Experimental Procedures in the presence of 1 μM transducin, 25 μM PDEγ-(63−87), 0.5 μM RGS9-1·Gβ5L, and either V8-uROS or uROS containing 20 μM rhodopsin. The recombinant trihelical domain of R9AP (abbreviated R9AP H1,2,3) (20 μM) was added where indicated. k_{GAP} was calculated as described in the legend of Figure 4. The data were taken from one of two independent experiments; error bars represent the standard error of the mean.

DISCUSSION

Complementary Regulation of RGS9-1·Gβ5L by PDEγ and R9AP. RGS9-1·Gβ5L plays an essential role in regulating the temporal resolution of vision. Its knockout causes slow photoresponse recovery in mice (*25*, *26*), and in humans, its mutations result in difficulties adjusting to bright light and an impaired ability to see moving objects (*27*). The activity of RGS9-1·Gβ5L is tightly controlled by two proteins, transducin's effector, the γ-subunit of cGMP phosphodiesterase (PDEγ) (*28*), and the membrane anchor, R9AP (*6*, *8*, *9*). Regulation of RGS9-1·Gβ5L by each of these proteins occurs through complementary yet nonoverlapping mechanisms.

PDEγ contributes to the substrate specificity of RGS9-1·Gβ5L. The affinity of RGS9-1·Gβ5L for transducin complexed with PDEγ is much higher than that for free activated transducin (*16*). Therefore, PDEγ acts as an affinity adapter, setting up a situation which favors transducin inactivation only after it has a chance to activate the effector (*29*). Meanwhile, R9AP enhances the maximal speed at which RGS9-1·Gβ5L can activate transducin GTPase. We have now demonstrated R9AP causes only a minor enhancement in the affinity between RGS9-1·Gβ5L and transducin, whereas the major effect is based on modulating the catalytic efficiency of RGS9-1·Gβ5L.

Activation of RGS9-1·Gβ5L by R9AP enables it to stimulate the GTPase activity of transducin at a rate of ~40 turnovers/s (Figure 1) and likely faster at body temperature. The physiological significance of this rate can be illustrated by the fact that under normal daylight conditions of illumina-

tion the human eye can detect a flicker frequency of at least 60 Hz (*30*). As such, most people find it uncomfortable to use CRT computer monitors set at refresh rates of <70 Hz because only at this or higher refresh rates do individual frames completely merge into one steady image. This implies that each individual photoreceptor response to light starts turning off at a comparable rate. On the molecular level, this requires an appreciable degree of transducin inactivation within just ~15 ms after the onset of the photoresponse, a rate that can be achieved only when RGS9-1·Gβ5L is activated by R9AP.

Possible Implications of Elucidating the Kinetic Mode of R9AP Action for Understanding General Principles of RGS Protein Function. Our findings may contribute to the understanding of the general mechanism by which RGS proteins activate G protein GTPase. It is well-established that RGS proteins interact most efficiently with G protein α-subunits in their transition state for GTP hydrolysis and stimulate GTP hydrolysis by stabilizing this conformation (see ref *31* for a review). What is not clear is whether RGS proteins can trap α-subunits only after the latter assume the transition state or whether the transition state can be actively induced upon this interaction. Our kinetic data support the second possibility. We have shown that at *saturating* concentrations of transducin, when essentially all RGS9-1·Gβ5L is bound to transducin, RGS9-1·Gβ5L associated with R9AP stimulates transducin GTPase much more rapidly than RGS9-1·Gβ5L without R9AP. This suggests that the transition state of the transducin α-subunit is either induced or preserved more efficiently when RGS9-1·Gβ5L is bound to R9AP.

Understanding the molecular details of regulation of RGS9-1·Gβ5L by R9AP remains a goal for future studies. The fact that the minimal RGS9-1 binding domain of R9AP is insufficient for RGS9-1·Gβ5L activation suggests a couple of interesting hypotheses. One is that R9AP has two functional domains, one that binds RGS9-1·Gβ5L and another that directly interacts with transducin to help stimulate its GTPase activity. Another is that potentiation is only possible when R9AP holds RGS9-1·Gβ5L on the membrane surface (and also on detergent micelles, given the data from Figure 5B) and that secondary interactions with lipids help RGS9-1·Gβ5L to assume the conformation optimal for activating transducin GTPase.

Our findings may also facilitate the studies of the recently discovered brain-specific homologue of R9AP, R7BP (*32*, *33*). R7BP interacts with RGS9-1 and three other closely related RGS proteins, RGS6, RGS7, and RGS11, both in vivo and in vitro. Much like R9AP in photoreceptor cells, R7BP was suggested to control the membrane association of its RGS protein partners in other neurons (*33*, *34*). Determining if R7BP can also modulate RGS protein activity is another challenge for future experiments.

REFERENCES

1. Burns, M. E., and Arshavsky, V. Y. (2005) Beyond counting photons: Trials and trends in vertebrate visual transduction, *Neuron 48*, 387−401.
2. Fung, B. K., Hurley, J. B., and Stryer, L. (1981) Flow of information in the light-triggered cyclic nucleotide cascade of vision, *Proc. Natl. Acad. Sci. U.S.A. 78*, 152−6.
3. He, W., Cowan, C. W., and Wensel, T. G. (1998) RGS9, a GTPase accelerator for phototransduction, *Neuron 20*, 95−102.
4. Makino, E. R., Handy, J. W., Li, T., and Arshavsky, V. Y. (1999) The GTPase activating factor for transducin in rod photoreceptors is the complex between RGS9 and type 5 G protein β subunit, *Proc. Natl. Acad. Sci. U.S.A. 96*, 1947−52.
5. Hu, G., and Wensel, T. G. (2002) R9AP, a membrane anchor for the photoreceptor GTPase accelerating protein, RGS9-1, *Proc. Natl. Acad. Sci. U.S.A. 99*, 9755−60.
6. Martemyanov, K. A., Lishko, P. V., Calero, N., Keresztes, G., Sokolov, M., Strissel, K. J., Leskov, I. B., Hopp, J. A., Kolesnikov, A. V., Chen, C. K., Lem, J., Heller, S., Burns, M. E., and Arshavsky, V. Y. (2003) The DEP domain determines subcellular targeting of the GTPase activating protein RGS9 in vivo, *J. Neurosci. 23*, 10175−81.
7. Keresztes, G., Martemyanov, K. A., Krispel, C. M., Mutai, H., Yoo, P. J., Maison, S. F., Burns, M. E., Arshavsky, V. Y., and Heller, S. (2004) Absence of the RGS9·Gβ5 GTPase-activating complex in photoreceptors of the R9AP knockout mouse, *J. Biol. Chem. 279*, 1581−4.
8. Lishko, P. V., Martemyanov, K. A., Hopp, J. A., and Arshavsky, V. Y. (2002) Specific binding of RGS9-Gβ5L to protein anchor in photoreceptor membranes greatly enhances its catalytic activity, *J. Biol. Chem. 277*, 24376−81.
9. Hu, G., Zhang, Z., and Wensel, T. G. (2003) Activation of RGS9-1 GTPase acceleration by its membrane anchor, R9AP, *J. Biol. Chem. 278*, 14550−4.
10. McDowell, J. H. (1993) Preparing Rod Outer Segment Membranes, Regenerating Rhodopsin, and Determining Rhodopsin Concentration, *Methods Neurosci. 15*, 123−30.
11. Nekrasova, E. R., Berman, D. M., Rustandi, R. R., Hamm, H. E., Gilman, A. G., and Arshavsky, V. Y. (1997) Activation of transducin guanosine triphosphatase by two proteins of the RGS family, *Biochemistry 36*, 7638−43.
12. Bownds, D., Gordon-Walker, A., Gaide-Huguenin, A. C., and Robinson, W. (1971) Characterization and analysis of frog photoreceptor membranes, *J. Gen. Physiol. 58*, 225−37.
13. Ting, T. D., Goldin, S. B., and Ho, Y.-K. (1993) Purification and Characterization of Bovine Transducin and Its Subunits, *Methods Neurosci. 15*, 180−95.
14. Skiba, N. P., Martemyanov, K. A., Elfenbein, A., Hopp, J. A., Bohm, A., Simonds, W. F., and Arshavsky, V. Y. (2001) RGS9-Gβ5 substrate selectivity in photoreceptors. Opposing effects of constituent domains yield high affinity of RGS interaction with the G protein-effector complex, *J. Biol. Chem. 276*, 37365−72.
15. Martemyanov, K. A., and Arshavsky, V. Y. (2004) Kinetic approaches to study the function of RGS9 isoforms, *Methods Enzymol. 390*, 196−209.
16. Skiba, N. P., Hopp, J. A., and Arshavsky, V. Y. (2000) The effector enzyme regulates the duration of G protein signaling in vertebrate photoreceptors by increasing the affinity between transducin and RGS protein, *J. Biol. Chem. 275*, 32716−20.
17. Arshavsky, V. Y., Dumke, C. L., Zhu, Y., Artemyev, N. O., Skiba, N. P., Hamm, H. E., and Bownds, M. D. (1994) Regulation of transducin GTPase activity in bovine rod outer segments, *J. Biol. Chem. 269*, 19882−7.
18. Krumins, A. M., and Gilman, A. G. (2002) Assay of RGS protein activity in vitro using purified components, *Methods Enzymol. 344*, 673−85.
19. Ramdas, L., Disher, R. M., and Wensel, T. G. (1991) Nucleotide exchange and cGMP phosphodiesterase activation by pertussis toxin inactivated transducin, *Biochemistry 30*, 11637−45.
20. Bokoch, G. M., Katada, T., Northup, J. K., Ui, M., and Gilman, A. G. (1984) Purification and properties of the inhibitory guanine nucleotide-binding regulatory component of adenylate cyclase, *J. Biol. Chem. 259*, 3560−7.
21. Higashijima, T., Ferguson, K. M., Sternweis, P. C., Smigel, M. D., and Gilman, A. G. (1987) Effects of Mg^{2+} and the $\beta\gamma$-subunit complex on the interactions of guanine nucleotides with G proteins, *J. Biol. Chem. 262*, 762−6.
22. Keresztes, G., Mutai, H., Hibino, H., Hudspeth, A. J., and Heller, S. (2003) Expression patterns of the RGS9-1 anchoring protein R9AP in the chicken and mouse suggest multiple roles in the nervous system, *Mol. Cell. Neurosci. 24*, 687−95.
23. Lerman, J. C., Robblee, J., Fairman, R., and Hughson, F. M. (2000) Structural analysis of the neuronal SNARE protein syntaxin-1A, *Biochemistry 39*, 8470−9.
24. Fernandez, I., Ubach, J., Dulubova, I., Zhang, X., Sudhof, T. C., and Rizo, J. (1998) Three-dimensional structure of an evolutionarily conserved N-terminal domain of syntaxin 1A, *Cell 94*, 841−9.

25. Chen, C. K., Burns, M. E., He, W., Wensel, T. G., Baylor, D. A., and Simon, M. I. (2000) Slowed recovery of rod photoresponse in mice lacking the GTPase accelerating protein RGS9-1, *Nature 403*, 557−60.
26. Krispel, C. M., Chen, C. K., Simon, M. I., and Burns, M. E. (2003) Prolonged photoresponses and defective adaptation in rods of Gβ5−/− mice, *J. Neurosci. 23*, 6965−71.
27. Nishiguchi, K. M., Sandberg, M. A., Kooijman, A. C., Martemyanov, K. A., Pott, J. W., Hagstrom, S. A., Arshavsky, V. Y., Berson, E. L., and Dryja, T. P. (2004) Defects in RGS9 or its anchor protein R9AP in patients with slow photoreceptor deactivation, *Nature 427*, 75−8.
28. Arshavsky, V., and Bownds, M. D. (1992) Regulation of deactivation of photoreceptor G protein by its target enzyme and cGMP, *Nature 357*, 416−7.
29. Arshavsky, V. Y., and Pugh, E. N., Jr. (1998) Lifetime regulation of G protein-effector complex: Emerging importance of RGS proteins, *Neuron 20*, 11−4.
30. Pieron, H. (1965) Vision in Intermittent Light. Laws and Mechanisms of the Critical Frequency for Fusion, *Contributions in Sensory Physiology 14*, 179−264.
31. Ross, E. M., and Wilkie, T. M. (2000) GTPase-activating proteins for heterotrimeric G proteins: Regulators of G protein signaling (RGS) and RGS-like proteins, *Annu. Rev. Biochem. 69*, 795−827.
32. Martemyanov, K. A., Yoo, P. J., Skiba, N. P., and Arshavsky, V. Y. (2005) R7BP, a novel neuronal protein interacting with RGS proteins of the R7 family, *J. Biol. Chem. 280*, 5133−6.
33. Drenan, R. M., Doupnik, C. A., Boyle, M. P., Muglia, L. J., Huettner, J. E., Linder, M. E., and Blumer, K. J. (2005) Palmitoylation regulates plasma membrane-nuclear shuttling of R7BP, a novel membrane anchor for the RGS7 family, *J. Cell Biol. 169*, 623−33.
34. Song, J. H., Waataja, J. J., and Martemyanov, K. A. (2006) Subcellular targeting of RGS9-2 is controlled by multiple molecular determinants on its membrane anchor, R7BP, *J. Biol. Chem. 281*, 15361−9.
35. He, W., Melia, T. J., Cowan, C. W., and Wensel, T. G. (2001) Dependence of RGS9-1 membrane attachment on its C-terminal tail, *J. Biol. Chem. 276*, 48961−6.

BI060376A